Notes

$K_8Tl_{10}Zn$: A Zintl Phase Containing the Zinc-Centered Thallium Polyanion $Tl_{10}Zn^{8-}$

Zhen-Chao Dong, Robert W. Henning, and John D. Corbett*

Ames Laboratory−DOE[1] and Department of Chemistry, Iowa State University, Ames, Iowa 50011

Received March 14, 1997

Introduction

Explorations of the alkali-metal−triel (A−Tr) systems have led to the discovery of many new materials with novel structural features and to many clear delineations of differences in chemistry among the elements Ga, In, and Tl.[2] Several of the network phases found contain classic deltahedral cluster units, interbridged octahedral In_6[3] and icosahedral Ga_{12}[4] for example, that are analogous to the clusters found in borane chemistry, but other types have been uncovered that are substantial alterations of regular deltahedra, In_{11}^{7-} ($\sim D_{3h}$)[5] and Tl_9^{9-} (C_{2v})[6] for instance. Wade's rules[7] have been very successful in correlating electron counts with structure not only for the boranes but also for certain clusters of gallium, indium, and thallium, but several new nonclassical examples do not conform. The phases K_8In_{11}[5] and A_8Tl_{11} (A = K−Cs)[8] for example contain pentacapped trigonal prismatic Tr_{11}^{7-} units that require only 40 electrons for stability while the classical closo polyhedron would need 48 electrons. Reduction in the overall charges on the clusters is believed to be a significant driving force behind the observed distortions. Another way to reduce the total electron count of a cluster is to bond an interstitial atom within. Such have been observed for indium in $K_8In_{10}Zn$[9] and $K_{10}In_{10}Ni$,[10] which contain isolated 10-atom clusters centered by zinc or nickel, as well as in several icosahedral $Tl_{12}M^{n-}$ examples.[11,12] As might be expected from comparisons of the chemistries of Ag and Au or Cd and Hg, the cluster chemistry of the triel elements In and Tl show a great many differences. To date 14 cluster compounds have been found that are unique to thallium and only two that are common to both, tetrahedral Tr_4^{8-} and the above Tr_{11}^{7-}.[2] We here report the first commonality for a centered cluster in $K_8Tl_{10}Zn$. It contains a comparable distorted bicapped antiprismatic Tl_{10} centered by zinc and also exhibits closed-shell bonding.

Experimental Section

Syntheses. All material handling was carried out in the nitrogen or argon environment of a glovebox. Stoichiometric amounts of the elements K (99.9%, Baker), Tl (99.998%, Johnson-Matthey), and Zn (99.999%, Cerac) (~250−600 mg total) were loaded into a tantalum tube that had already been welded on one end. The opposite end was tightly crimped and then arc-welded in an argon atmosphere. As before,[13] the container was then sealed into an evacuated fused silica jacket in order to prevent oxidation of the Ta at high temperatures.

The components in appropriate proportions were first heated to 600 °C, held at that temperature for 24 h, and then slowly cooled, conditions that worked well for the congruently melting $K_8In_{10}Zn$. This procedure clearly yielded the new $K_8Tl_{10}Zn$, but the Guinier powder pattern also showed the presence of KZn_{13} and K_8Tl_{11}. A study of the binary phase diagrams[14] suggested that the very incongruent separation of some KZn_{13} near 592 °C drove the system off stoichiometry and thus led to the formation of K_8Tl_{11} as well. Therefore, the liquid system was quenched in water from 600 °C, annealed at 200 °C for 2 weeks, and quenched in water. The Guinier pattern showed that the product was single-phase $K_8Tl_{10}Zn$ (≥95%). Analogous reactions with Cd or Na gave other products.

The same compound was first synthesized by utilizing Baker's "Analyzed" zinc. However, this product showed an unusually large paramagnetic susceptibility plus an antiferromagnetic-like transition near −90 K. These effects were provisionally attributed to traces of some Fe−Zn product arising from 0.05 wt % Fe listed for the zinc reactant. A switch to the purer zinc source eliminated the problem.

Structure Determination. Selected crystallites were sealed into thin-walled glass capillaries and checked for singularity by Laue techniques. A suitable crystal ~0.13 × 0.13 × 0.11 mm was used for data collection on a Rigaku AFC6R diffractometer with graphite-monochromated Mo Kα radiation. A random search located 25 reflections that indexed to a tetragonal unit cell. Two octants of data ($h,k,\pm l$) were collected at 23 °C up to $2\theta = 55°$. A total of 3700 reflections were measured and subsequently corrected for Lorentz and polarization effects and for a sizable absorption ($\mu = 569$ cm^{-1}) with the aid of the average of four ψ-scan curves. An unambiquous space group assignment *P*4/*nnc* (No. 126) was made on the basis of the Laue symmetry determined by the diffractometer programs, the systematic absences, and the Wilson statistics.

The beginning of the structural solution was via direct methods,[15] which provided two large peaks with separations appropriate for bonded thallium atoms. Least-squares refinement and difference Fourier analysis revealed two more positions that were appropriate for zinc and potassium. DIFABS was applied as recommended[16] after full isotropic refinement to improve the relatively large absorption correction. The anisotropic refinement utilized 300 independent reflections ($I \geq 3\sigma_I$) and 25 variables (including a secondary extinction coefficient) and converged at $R(F) = 3.7\%$ and $R_w = 3.6\%$ with a GOF = 1.07. All calculations were handled on a VAX station using the TEXSAN[17] crystallographic package. A selection of data collection parameters is tabulated in Table 1, atomic positions and isotropic-equivalent displacement parameters are listed in Table 2, and relevant bond distance data are given in Table 3. A more detailed summary and the anisotropic displacement parameters are included in the Supporting Information. These as well as the structure factor data are also available from J.D.C.

Magnetic Measurements. Magnetic susceptibility data were obtained with the aid of a Quantum Design MPMS SQUID magnetometer over the temperature range 6−300 K at a field of 3 T. A 51.3-mg powdered sample was loaded inside a helium-filled glovebox into a container[18] that held the sample between two fused silica rods and within a third tube, and the assembly was then sealed. The raw data were corrected for the susceptibility of the sample holder, the diamagnetic

(1) This research was supported by the Office of the Basic Energy Sciences, Materials Sciences Division, U.S. Department of Energy. The Ames Laboratory is operated by Iowa State University under Contract No. W-7405-Eng.82.

(2) Corbett, J. D. In *Chemistry, Structure and Bonding of Zintl Phases and Ions*; Kauzlarich, S, Ed.; VCH Publishers: New York, 1996; Chapter 3.
(3) Sevov, S. C.; Corbett, J. D. *Z. Anorg. Allg. Chem.* **1993**, *619*, 128.
(4) Ling, R. G.; Belin, C. *Acta Crystallogr.* **1982**, *B38*, 1101.
(5) Sevov, S. C.; Corbett, J. D. *Inorg. Chem.* **1991**, *30*, 4875.
(6) Dong, Z.-C.; Corbett, J. D. *Inorg. Chem.* **1996**, *35*, 3107.
(7) Wade, K. *Inorg. Chem. Radiochem.* **1976**, *18*, 1.
(8) Dong, Z.-C.; Corbett, J. D. *J. Cluster Sci.* **1995**, *6*, 187.
(9) Sevov, S. C.; Corbett, J. D. *Inorg. Chem.* **1993**, *32*, 1059.
(10) Sevov, S. C.; Corbett, J. D. *J. Am. Chem. Soc.* **1993**, *115*, 9080.
(11) Dong, Z.-C.; Corbett, J. D. *J. Am. Chem. Soc.* **1995**, *117*, 6447.
(12) Dong, Z.-C.; Corbett, J. D. *Angew. Chem., Int. Ed. Engl.* **1996**, *35*, 1006.
(13) Sevov, S. C.; Corbett, J. D. *Inorg. Chem.* **1992**, *31*, 1895.
(14) Massalski, T. B., Ed. *Binary Alloy Phase Diagrams*; ASM International: Materials Park, OH, 1990; Vol. 3, pp 2397, 2509.
(15) Sheldrick, G. M. SHELXS-86, Universität Göttingen, Germany, 1986.
(16) Walker, N.; Stuart, D. *Acta Crystallogr.* **1983**, *A39*, 158.
(17) *TEXSAN*, version 6.0; Molecular Structure Corp.: The Woodlands, TX, 1990.
(18) Guloy, A. M.; Corbett, J. D. *Inorg. Chem.* **1996**, *35*, 4670.

S0020-1669(97)00309-1 CCC: $14.00

Table 1. Summary of Data Collection and Refinement Parameters for $K_8Tl_{10}Zn$

fw	2421.87
lattice params, Å[a]	$a = 10.319(2)$
	$c = 13.859(3)$
V, Å^3	1475.7(5)
space group, Z	$P4/nnc$ (No. 126), 2
d_{calc}, g/cm^3	5.450
μ, cm^{-1} (Mo Kα)	568.7
transm coeff range	0.629−1.000
temp, °C	23
residuals: R; R_w[b]	0.037; 0.036

[a] From 37 lines in Guinier powder pattern with Si as an internal standard, $\lambda = 1.540\,562$ Å, $T = 23$ °C. [b] $R = \sum||F_o| - |F_c||/\sum|F_o|$; $R_w = [\sum w(|F_o| - |F_c|)^2/\sum w(F_o)^2]^{1/2}$, $w = 1/\sigma_F^2$.

Table 2. Positional Coordinates and Isotropic Thermal Parameters for $K_8Tl_{10}Zn$

atom	Wyckoff	x	y	z	B_{eq} (Å^2)[a]
Tl1	16*k*	0.8448(1)	0.9892(1)	0.3392(1)	2.19(6)
Tl2	4*e*	1/4	1/4	0.5398(2)	2.70(7)
Zn	2*b*	1/4	1/4	3/4	1.4(2)
K	16*k*	0.8223(8)	0.0460(8)	0.6058(6)	3.1(4)

[a] $B_{eq} = (8\pi^2/3)\sum_i\sum_j U_{ij}a_i^*a_j^*\vec{a}_i\vec{a}_j$.

Table 3. Atom Separations in $K_8Tl_{10}Zn$ (<5 Å)

Tl1−Tl1	3.153(3)	Zn−Tl1 (8×)	2.928(1)
Tl1−Tl1	3.248(3)	Zn−Tl2 (2×)	2.913(3)
Tl1−Tl1[a] (2×)	3.755(2)	K−Tl1[b]	3.537(9)
Tl1−Tl2	3.140(2)	K−Tl1	3.697(9)
Tl1−Zn	2.928(1)	K−Tl1[b]	3.725(9)
Tl1−Kb	3.537(9)	K−Tl1	3.749(8)
Tl1−K[c]	3.697(9)	K−Tl1	3.939(8)
Tl1−K[b]	3.725(9)	K−Tl2	3.736(8)
Tl1−K[d]	3.749(8)	K−K	4.27(2)
Tl1−K[e]	3.939(8)	K−K (2×)	4.31(1)
Tl2−Tl1 (4×)	3.140(2)	K−K (2×)	4.45(1)
Tl2−Zn	2.913(3)	K−K	4.47(2)
Tl2−K (4×)	3.736(8)		

[a] Within square base. [b] Bridges on same square. [c] Exo-bonding. [d] Bridging to Tl2. [e] Between square units.

core electrons, and the Larmor precession contribution of the delocalized electrons in the cluster valence orbitals.[5,6] The latter two terms amounted to -4.54×10^{-4} and -3.43×10^{-4} emu/mol, respectively.

Calculations. Extended Hückel tight-binding computations were carried out with the aid of Gordon Miller's local modification of the EHMACC suite of programs written at Cornell University by various member of the R. Hoffmann group. These employed H_{ii} (ev) and ξ values as follows: Tl 6s, −11.60, 2.14; 6p, −5.80, 2.04; Zn 4s, −l2.41, 2.01; 4p, −6.53, l.70.

Discussion

The primary structural feature of gray reflective $K_8Tl_{10}Zn$ is the classic bicapped square antiprism of thallium (as in $B_{10}H_{10}^{2-}$) that is now centered by zinc, Figure 1. (The entire cell is illustrated in the Table of Contents.) The ideal cluster is compressed along the axial direction, and the capped squares expanded to produce nearly equidistant Zn−Tl separations, Zn−Tl1, 2.928(1) Å and Zn−Tl2 (axial), 2.913(3) Å. A slight twist (1.74°) between the two square faces of the antiprism leads from the ideal D_{4d} to D_4 symmetry and to two different Tl1−Tl1 contacts, 3.153(3) and 3.248(3) Å. The distortion is probably caused by packing effects from the 42 symmetry of the cations. As has been characteristic of cation−cluster interactions,[2] the K atoms sheath the cluster in three different modes, Figure 2, and each K contacts three clusters. The single type of potassium thus caps each of the eight Tl1 triangular faces around the cluster at 3.537(9)−3.939(8) Å, bridges all Tl1−Tl2 edges, 3.736(8)−3.749(8) Å, and bonds exo to the eight Tl1 atoms at 3.697(9) Å but not at the pair of Tl2 vertices. The face capping modes are somewhat distorted in that the two rings of capping atoms about the waist, Figure 2, have moved away from one another. The 24 multifunctioned potassium atoms about each cluster thus serve to isolate these from each other. The closest contact between the polyanions is 5.494(3) Å (Tl1−Tl1).

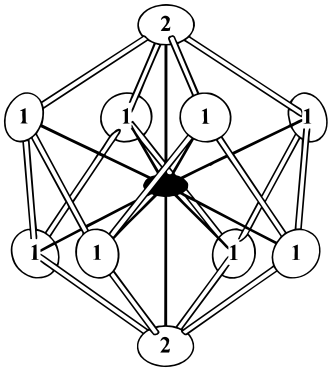

Figure 1. Isolated $Tl_{10}Zn^{8-}$ cluster with thermal ellipsoids drawn at 90% probability.

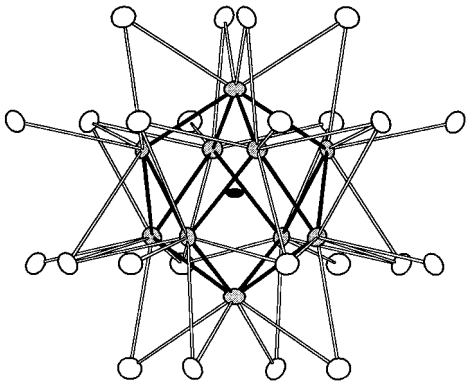

Figure 2. The $Tl_{10}Zn^{8-}$ cluster with the 24 potassium neighbors (μ_3, μ_2, μ_1).

Extended Hückel calculations on the isolated cluster indicate that, as in the isostructural $K_8In_{10}Zn$,[5] 20 skeletal electrons are needed for stability, as follows. The $6s^2$ pair on each thallium form a collection of low-lying MOs and can be viewed as lone pairs at each vertex. The bicapped antiprism requires only 2*n* electrons once the square faces of the antiprism have been expanded (3.76 Å on edge). The valence s and p orbitals on $4s^2$ Zn interact with respective filled a_1 (s), e_1 (p_x, p_y), and b_2 (p_z) cluster MO's and stabilize these. The pair of filled a_1 orbitals interact strongly, and the a_1* result is driven high and emptied, leaving a 2*n* skeletal electron requirement for the $n = 10$ polyhedron. The 20 bonding skeletal electrons originate with 10 Tl (1 each), Zn (2), and the cations (8) and achieve a closed-shell Zintl phase. The overall process is apparently favored because, in addition to the gain of central Tl−Zn bonding (there are no Tl−Zn binary compounds for comparison[14]), a cluster is created with four fewer charges than would be needed in a classical *closo*-Tl_{10}^{12-}, all at the expense of only one cluster bonding MO. Of course, the Coulomb energy associated with the assembly of the cluster anion and solvating cations is certainly a major factor in the absolute stability of the compound.[2]

The new $K_8Tl_{10}Zn$ is appropriately diamagnetic, Figure 3, a feature that also pertains to the particularly stable $K_8In_{10}Zn$,[9] $K_{10}In_{10}Ni$,[10] $K_8In_{10}Hg$,[19] and $Cs_8Ga_{11}Cl$.[20] The last two are not centered but closed-shell derivatives of the odd-electron $A_8Tr_{11}(e^-)$

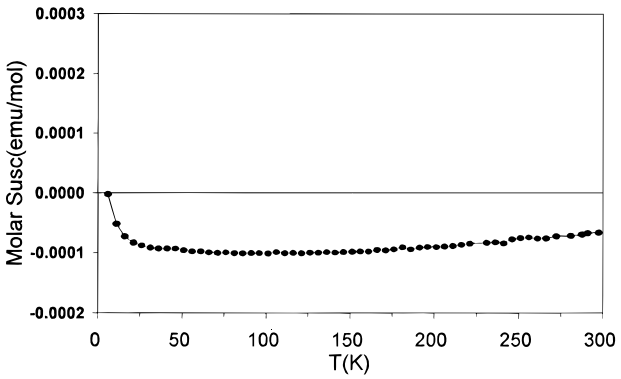

Figure 3. Magnetic susceptibility of $K_8Tl_{10}Zn$ at 3 T.

family. The corresponding gallium−zinc compound has not been observed; rather, K_2Ga_3[21] is the predominant product in reactions loaded as $K_8Ga_{10}Zn$ while $Na_{22}Ga_{39}$[22] forms in the sodium system.

An interesting similarity is found among the 11-atom clusters $Tl_{10}Zn^{8-}$, $In_{10}Zn^{8-}$, and the previously reported Tl_{11}^{7-},[8] In_{11}^{7-},[5] and $In_{10}Ni^{10-}$.[10] Even though the overall cluster geometries are different, each of the three types of clusters requires 40 (skeletal and lone pair) electrons for stability. The isoelectronic nickel derivative can be regarded as an alternative C_{3v} cluster favored by the need to bind a greater number of cations.[10] The nickel interstitial has two fewer electrons than zinc, and this is compensated by a correspondingly 2− greater charge on the cluster. The Tr_{11}^{7-} species are not centered, but they still have the same total of atoms in the cluster unit and represent the homoatomic version that is most hypoelectronic ($2n - 4$) relative to Wade's rules ($2n + 2$). Melting properties (see Experimental Section) indicate the present $K_8Tl_{10}Zn$ is thermodynamically distinctly less stable than $K_8In_{10}Zn$ with respect to neighboring phases, which are comparable in both cases.

Acknowledgment. The authors thank J. Ostenson for the magnetic susceptibility data and G. J. Miller for the extended Hückel program.

Supporting Information Available: Two files of data collection and refinement information and the anisotropic displacement parameters, in CIF format, are available. Access information is given on any current masthead page.

IC970309S

(19) Sevov, S. C.; Corbett, J. D.; Ostenson, J. E. *J. Alloys Compd.* **1993**, *202*, 289.
(20) Henning, R. W.; Corbett, J. D. Unpubished research.
(21) Tillard-Charbonnel, M.; Chouaibi, N.; Belin, C., *C. R. Hebd. Seances Acad. Sci., Ser. II* **1990**, *311*, 69.
(22) Ling, R. C.; Belin C. *Acta Crystallogr.* **1982**, *B38*, 1101.